Characterization Studies of Reduced Graphene Oxide/Zinc Oxide Nanocomposites Synthesized by Hydrothermal Method

A. A. Ebnalwaled [1], A. Abu El-Fadl [2] *, Muhammad A. Tuhamy[2]

1. Department of Physics, Faculty of Science, South Valley University, Qena 83523, Egypt
2. Department of Physics, Faculty of Science, Assiut University, Assiut 71516, Egypt
E-mail: abulfadla@yahoo.com

Abstract: Reduced graphene oxide/zinc oxide (RGO/ZnO) nanocomposites were synthesized by facile hydrothermal method; this method consists of exfoliation of graphite with modified Hummer's method and synthesis of (RGO/ZnO) nanocomposites using hydrothermal method. X-ray diffraction, TEM and FT-IR spectroscopy were used for structure morphological characterization. Optical properties of the samples were studied by measuring their optical absorbance. It can be concluded from XRD analysis that there are improvements of crystallinity associated with the increase of the crystallite size, as well as the increase in both of the (Zn-O) bond length and unit cell volume with the increase of ZnO ratio in RGO/ZnO nanocomposites. The morphological studies confirmed that the scale of ZnO particles is large and the size distribution is not uniform in samples of RGO/ZnO and that most particles have average size of about 9 nm while some particles even have larger size. The optical absorption spectra show that the excitonic peak of the as-prepared samples is red shifted from 268 nm to 376 nm for reduced grapheme oxide (RGO) with the increase of ZnO ratio, and the optical band gap changes from 2.39 for pure RGO to 3.34 eV for pure ZnO. The effect of UV irradiation on the optical absorption nanocomposites at different UV doses was carried out using UV lamp.

Keywords: Reduced graphene oxide; Hydrothermal; Hummer's method; RGO/ZnO nanocomposites; optical energy gap; UV irradiation.

1. Introduction

ZnO nanomaterials are attractive candidates for fabricating biosensors, super capacitors, solar cells, and another several electronic devices because of their diverse range of nanostructures, high electron mobility, chemical stability, and electrochemical activity, high isoelectric points which promote enzyme adsorption, bio compatibility, and piezoelectric properties [1]. Graphene which is a new important member in the family of carbon can be described as mono layer or a few layers of 2D planar sheet of sp^2 hybridized carbon atoms arranged in a hexagonal lattice was first synthesized by modified Hummer's method [2]–[4]. It is a very good choice for electrode because of its characteristics, like excellent electrical conductivity, fast electron mobility, high surface area to volume ratio, and very good thermal and electrochemical properties [5]. Graphene has been widely studied for use in many electronics applications, due to its large theoretical surface area, good electronic conductivity, mechanical properties, and exceptional thermal stability, high electrical activity, good optical transmittance [6]. Graphene as a new member of the family of carbon can be used as an ideal choice for preparing nanocomposites like metal oxides, metal sulfides and metal nanoparticles for improved properties. The graphene based materials are widely used in several applications like, photo catalysis [7], energy storage, gas sensors [3]and biosensors [3], [8]–[12], light emitting diodes (LED) [13] Graphene and other carbon-based materials show a good conductivity when they coupled with metal oxides [14].

Reduced Graphene oxide has been synthesized by different methods such as chemical vapor deposition (CVD), micro mechanical exfoliation, epitaxial growth, thermal reduction and chemical methods (modified Hummer method) [2], [15]. Among those methods Hummer's method and it's modifies are the most used methods [16].

Among the many metal oxides, zinc oxide (ZnO) is the most attractive as a promising material because of its low cost, rich availability, environmental friendly nature and electrochemical activity and direct wide band-gap about 3.37 eV [1]. RGO/ZnO nanocomposites may exhibit unique properties due to the interactive effect between graphene and ZnO for improved electrical conductivity and electron transfer rate (electron mobility) [17]. The attracting properties of RGO/ZnO nanocomposites have been widely studied like enhanced photo catalytic performance [18], energy storage capability, sensing property, optoelectronic property and ultra-fast nonlinear optical switching ability [19].
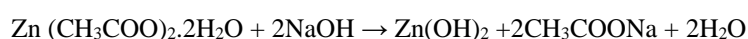
In the present investigation reduced graphene oxide synthesized by modified Hummer's method, Zinc oxide synthesized by hydrothermal method, and RGO/ZnO nanocomposites were synthesized by hydrothermal method and various characterization techniques have been employed to investigate the structure, morphology and optical absorption spectra for the prepared samples.

2. Experimental

2.1 Materials

Graphite powder (99%) and hydrazine hydrates purchased from Fisher Scientific, (United Kingdom), zinc acetate dihydrate ($(CH_3COO)_2Zn_2.H_2O$) (98%) purchased from Oxford Laboratory Reagent, India, sodium hydroxide pellets (NaOH) purchased from Fisher Scientific, United Kingdom, potassium permanganate ($KMnO_4$) (99%), sulfuric acid (98%), hydrochloric acid (HCl) (38%) and hydrogen peroxide (H_2O_2) (30%) purchased from El-Nasr Pharmaceutical Chemical Egypt. All the commercial chemical reagents which used in this experiment were used without further precipitation and distilled water was used in all experiment.

ZnO nanoparticles were prepared according to equations (1), (2) and the residual sodium salt CH_3COONa was removed by washing the sample with absolute ethanol and distilled water for several times [15], [16], [19].

$$Zn\ (CH_3COO)_2.2H_2O + 2NaOH \rightarrow Zn(OH)_2 + 2CH_3COONa + 2H_2O$$

$$Zn(OH)_2 + 2H_2O \rightarrow Zn(OH)_4^{-2} + 2H^+ \tag{1}$$

$$Zn(OH)_4^{-2} \rightarrow ZnO + H_2O + 2OH \tag{2}$$

2.2 Preparation of reduced graphene oxide (RGO)

Reduced graphene oxide in nano form prepared via modified Hummer's method. Reduced graphene oxide (RGO) synthesis can be distinguished into two major steps, firstly oxidation of graphite flakes into exfoliated graphene oxide (GO) and reduction GO into RGO. Starting with graphite powder washed with hydrochloric acid (HCl) then washed with distilled water several times, then the powder dissolved in concentrated sulfuric acid. Soft potassium permanganate added wisely to the solution, the solution temperature must be less than 20 °C by putting the mixture in ice bath. After stirring for 45 minutes the mixture diluted by adding wisely 100 mL of distilled water. The mixture heated up to 90°C then 40 mL of hydrogen peroxide was added, after stirring for 30 minutes the mixture let a night to precipitate and washed by HCl then washed several times by distilled water and then the powder was filtered and graphite oxide powder was obtained [3], [4], [16], [20]. Graphite oxide powder was dissolved in distilled water and the black suspension transferred into sonication (50 Hz) for 180 min at room temperature to exfoliate the stacked graphite oxide sheets into graphene oxide (GO), then the black suspension centrifuged for 30 min at 1000 rpm to remove the aggregation from graphene oxide also to remove the unexfoliated graphite, then the powder was filtered and washed by distilled water and ethanol several times, and dried at 100°C. The second step to obtain reduced graphene oxide is reducing the obtained graphene oxide by adding 0.5 g of the obtained GO to 1000 mL of distilled water and 5mL of hydrazine hydrate then the mixture transferred into reflux system at 100°C for 24 h. to reduce graphene oxide into reduced graphene oxide (removing oxygen containing groups). For 24 hours then suspension washed several times by distilled water then filtered and dried at 100°C to obtain RGO.

2.3 Preparation of reduced graphene oxide (RGO) /zinc oxide (ZnO) nanocomposites

Reduced graphene oxide (RGO) powder and zinc acetate in different ratios as shown in table 1 are dissolved in water and stirred for 15 min, then 1M of NaOH dropped wisely to the mixture until achieve pH= 10 and the white mixture was transferred into Teflon autoclave hydrothermal system for 24 h at 100 °C, then the product powder was filtered and washed by distilled water and ethanol, then dry at 100 °C.

Table 1. Different mass ratios of reduced graphene oxide to zinc oxide precursors used to form RGO/ZnO nanocomposites.

Name	Mass of RGO (g)	Mass of zinc acetate (g)	Weight ratio of RGO:Zn
ZnO	0	5	0:1
RGO	1	0	1:0
G/Zn1	1	1	1:1
G/Zn2	1	2	1:2
G/Zn3	1	3	1:3
G/Zn4	1	4	1:4
G/Zn5	1	5	1:5

2.4 Instrumentation and characterizations

The phase and crystalline size of the prepared samples were characterized using an automated X-ray powder diffractometer (Philips diffractometer 1710 with Cu target and graphite monochromator with the incident wavelength of 0.15418 nm). The morphological studies of samples were carried out using a transmission electron microscope (TEM) [JEOL JEM 1010] Japan performed at acceleration voltage of 200 KV].

Fourier transform infrared spectroscopy (FT-IR) analysis was carried out on a (Jasco Model-4000 Japan) 360 spectrometer to determine the specific functional groups present in the sample by KBr method.

UV-VIS spectrophotometer, UV2300, TECNOMOP was used to measure the absorbance, and transmittance of the prepared samples with wavelength scan from 190 to 1100 nm.

The UV irradiation at different exposure time (t) with the same concentration of colloidal solution were studied using Cole-Parmer 6-watt UV Lamp with 365 nm Wavelength and White Light Tubes.

3. Results and discussion

3.1 Structural studies

The crystalline structures, crystal size and phase purity of RGO, ZnO powders, and RGO/ZnO nanocomposites in different ratios were studied using XRD. The XRD patterns of the as synthesized pure ZnO and Pure RGO are shown in Fig. 1. (a) The XRD patterns of the synthesized (RGO/ZnO) nanocomposites materials are shown in Fig. 1. (b). XRD patterns were calculated in the range of 20° to 80° with step 0.06°. XRD main peaks are shown in Fig. 1. (a) indicate the presence of highly crystalline ZnO nanoparticles with a hexagonal structure (ICDD card no: 00-001-1136) with calculated d-spacing of 2.7 Å and a=b=2.5Å and c=3.99Å. Zinc oxide main peaks are sharp and confirming high crystallinity of the samples with main peak at 2θ=36.52º (101). These peaks correspond to (100), (002), (101), (102), (110), (103), (200), (112), and (201) crystalline planes related to the standard data of the ZnO. It is observed that peaks corresponding ZnO crystalline phase were detected in the XRD patterns of the samples with 2Θ values (31.977°, 34.64°, 36.52°, 47.77°, 56.833°, 63.096°, 66.607°, 68.181°, 69.31°, 72.804°, 77.182°, 81.52°, 89.823°) with hexagonal structure. Although in Graphene Main peaks are existed at 2θ=26.324°, 42.28°, 44.32°, 54.411°, and 72.16° with hexagonal structure (ICDD card no: 00-001-0640) corresponding to d-spacing of 2.799 Å, a=b= 3.506Å and c=5.598Å.

Fig. 1. (b) show that Zinc oxide main characterizing peaks appear with small intensity at RGO/Zn1 then the peaks intensity increase directly through different weight ratios from RGO/Zn1 to RGO/Zn5 although the intensity of graphene characterizing main peak are decreased. Fig. 2 shows the graphene main characterizing peak in different composite ratios was shifted to right with the increasing of zinc oxide content in the composite. The strong and sharp zinc oxide characterizing peaks in RGO/ZnO nanocomposites tell us that the ZnO nanoparticles stacked to graphene nanosheets are still crystalline as in the pure sample.

(a)   **(b)**
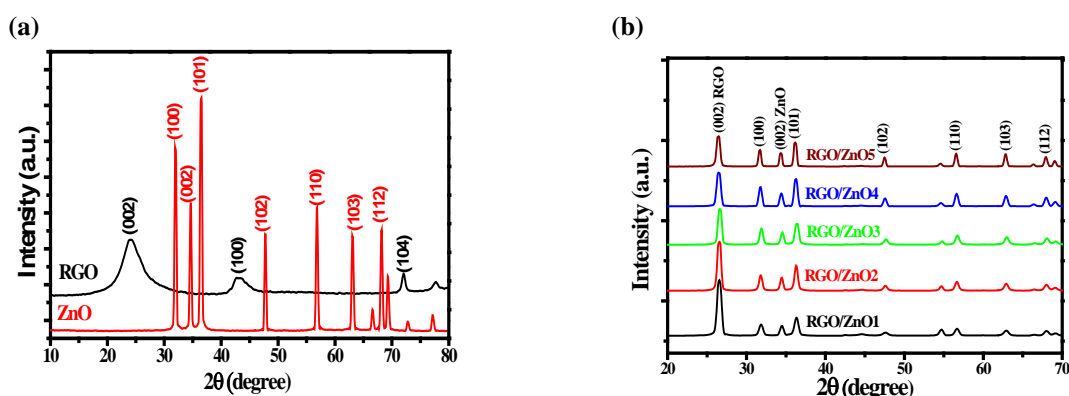
Fig. 1. (a) XRD patterns for pure reduced graphene oxide (RGO) and pure zinc oxide (ZnO), (b) XRD patterns for RGO/ZnO nanocomposites.

The lattice constants a, and c of a hexagonal plane for ZnO, RGO and RGO/ZnO nanocomposites are calculated using the following equation:

$$\frac{1}{d^2} = \frac{4}{3}\left(\frac{h^2+hk+k^2}{a^2}\right) + \frac{l^2}{c^2} \tag{3}$$

For hexagonal crystal system the unit cell volume can be calculated using the formula:

$$V = 0.866\ a^2 c \tag{4}$$

In the other hand the bond length (L) can be evaluated by the equation:

$$L = \sqrt{\frac{a^2}{3} + \left(\frac{1}{2} - z\right)^2 c^2}\ , \text{ where } z = \frac{a^2}{3} + \frac{1}{4} \tag{5}$$
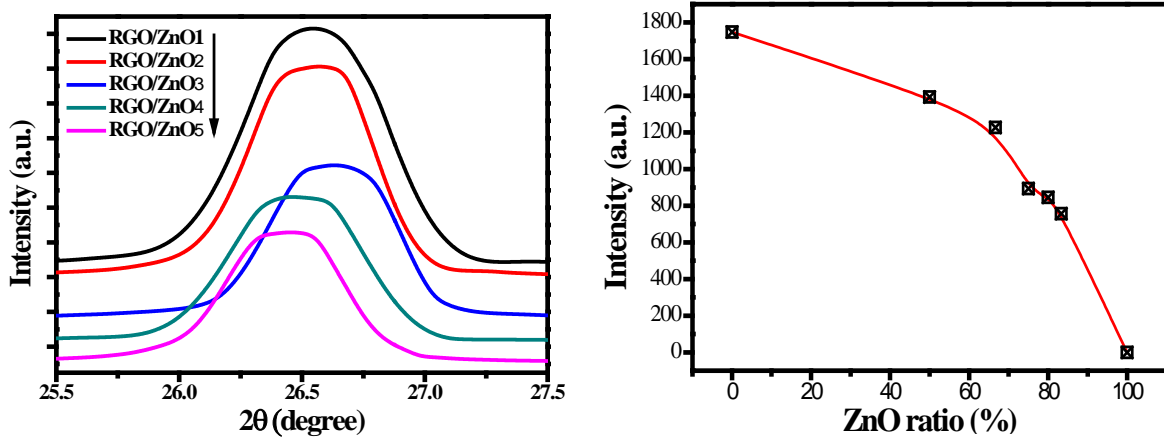
Fig. 2. The peak shift of (002) crystalline plane of RGO/ZnO nanocomposites.

The average particle sizes can be estimated from the maximum intensity peak corresponding to (002) plane by using Debye–Scherrer's formula according to the following equation [21]:

$$D_{hkl} = \frac{0.94\lambda}{\beta_{hkl}\cos\theta} \tag{6}$$

Where λ is the wavelength of the incident X-ray beams ($\lambda = 1.5418$ Å), θ is the diffraction angle, and β_{hkl} is the FWHM corrected for the instrumental broadening of the XRD peaks. It is found that the grain size of the samples is start with RGO about 8.8 nm in graphene and increases with increase of zinc oxide ratio in nanocomposites to reach about 22.5 nm in RGO/Zn5 and reaches 24.8 nm for pure ZnO sample. These findings indicate that the ZnO decorated on the RGO nanosheets in RGO/ZnO nanocomposites with a particle size ranges from 8.8 to 24.8 nm (according to the Debye–Scherer's formula). The increasing in grain size may be due to the increase in the both of Zn-O bond length and unit cell volume with increase in ZnO mass ratio (Fig. 3).
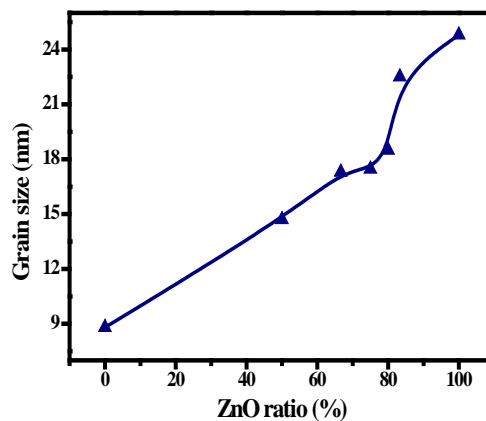
Fig. 3. The dependence of the grain size in RGO/ZnO nanocomposites with ZnO ratio.

Crystallite size and lattice strain is determined using Williamson-Hall (W-H) equation [22]:

$$\frac{\beta\cos\theta}{\lambda} = \frac{1}{D} + \frac{4\varepsilon\sin\theta}{\lambda} \tag{7}$$

where β is the full width at half maximum (FWHM), Θ is the diffraction angle, λ is X-ray wavelength, D is the crystalline size and ε is the lattice strain.

The dislocation density (δ) was calculated using the relation [23]:

$$\delta = 1/D^2 \tag{8}$$

According to Hook's law, for small dislocations in a lattice, a linear relation between the stress σ and strain is given as $\sigma = Y\,\varepsilon$, where Young's modulus Y (for hexagonal structure) can be represented by the following relation:

$$Y = \frac{\left(h^2 + \frac{(h+2k)^2}{3} + \left(\frac{al}{c}\right)^2\right)^2}{s_{11}\left(h^2 + \frac{(h+2k)^2}{3}\right) + s_{33}\left(\frac{al}{c}\right)^4 + (2s_{13} + s_{44})\left(h^2 + \frac{(h+2k)^2}{3}\right)\left(\frac{al}{c}\right)^2} \tag{9}$$

where s_{11}, s_{13}, s_{33}, s_{44} are the lattice compliances of ZnO which equal to 7.858×10^{-12}, -2.206×10^{-12}, 6.940×10^{-12}, and 23.57×10^{-12} m^2N^{-1} respectively. The energy density u (the energy per unit volume of a lattice) can be calculated from Hook's law $u = (\varepsilon^2 Y_{hkl})/2$. Values of ε, Y, σ, u, and the above-mentioned parameters of all samples are listed in table 2.

Table 2. The diffraction angle (2θ) value, crystallite size (D), lattice parameters (a, c and c/a), unit cell volume (V), internal local strain (ε), dislocation density (δ), Young modulus (Y), internal stress (σ), and energy density (u) for Reduced graphene oxide/zinc oxide (RGO/ZnO) nanocomposites (main peak).

Name	2θ of the main peak	D_{hkl} (nm)	Lattice parameter			V ($\mathring{A}^3$)	$\varepsilon \times 10^{-4}$ (radians)	$\delta \times 10^{15}$ (l/m^2)	$Y \times 10^{11}$ (Pascal)	$\sigma \times 10^8$ (Pascal)	$u \times 10^5$ (J/m^3)
			a ($\mathring{A}$)	c ($\mathring{A}$)	c/a						
ZnO	36.52	24.8	3.621	5. 78	1.596	65.6	14.6	1.62	2.47	3.6	5.26
RGO	26.324	8.8	3.192	5.103	1.596	44.9	75.9	12.9	2.36	17.9	135.1
G/Zn1	26.551	17.7	3.384	5.402	1.596	53.5	24.8	4.6	1.76	4.36	10.8
G/Zn2	26.541	17.3	3.465	5.432	1.596	57.5	20.9	3.31	1.83	2.89	8,38
G/Zn3	26.63	17.46	3.459	5.422	1.596	57.8	20.8	3.2	1.83	2.84	7.95
G/Zn4	26.48	18.5	3.469	5.538	1.596	57.7	20.1	2.9	1.84	2,68	5.68
G/Zn5	26. 43	22.5	3.566	5.693	1.596	62.69	16.3	1.9	1.84	2.41	3.9

The crystallite size D_{hkl} corresponds to main peak at $2\theta = 26.324°$ of the plane (002) in graphene and at $2\theta = 36.52°$ of the plane (101) in ZnO (other values recorded in table 2) was estimated using the Debye–Scherrer's formula.

3.2 Morphological Study

The TEM results manifest the transparent nature of the reduced graphene oxide indicating graphite was exfoliated into thin planar sheets and deposition of ZnO nanoparticles on the surface of the RGO sheets, which agree with the XRD pattern. Fig. 4(a, b, c) show TEM images with different magnifications for the three samples RGO, ZnO, and a selected ratio of the RGO/ZnO nanocomposite. It is clear to find that the scale of the ZnO particles is small (compared with RGO nanosheets) and the size distribution is not uniform in sample of RGO/ZnO and that most particles have average size of about 24 nm while some particles even have larger size and others has a smaller size. It is known that TEM uses both the transmitted and the scattered beams to create the image. As shown from Fig. 4 (a, b) the uniform size and shape distribution of ZnO obtained at low hydrothermal reaction time and temperature have semi-spherical shape. From the TEM the nano size of the obtained ZnO is confirmed with values obtained from XRD calculations.

3.3 Optical absorption studies

Optical absorption spectrum of RGO, ZnO, and RGO/ZnO nanocomposites samples were measured by UV-Vis spectrophotometer in the range 200-900 nm as shown in Fig. 5. (a, b, c). The figure depicted that for RGO there are main absorption peak at 246 nm and another shoulder at 299 nm which refer respectively to (C-C) and (C=C) bonds between the carbon atoms of reduced graphene oxide. In zinc oxide the main peak exists at 276 nm, but in RGO/ZnO nanocomposites in different ratios from RGO/ZnO1 to RGO/ZnO5 the exciton peak moved from 364

nm to 374 nm which mean that zinc oxide nanoparticles are stacked well on RGO nanosheets and the displacement in the peak is due to the difference in ZnO ratio which agree with the images obtained by TEM.

The corresponding excitonic energy (E_{ex}) can be calculated from the following formula:
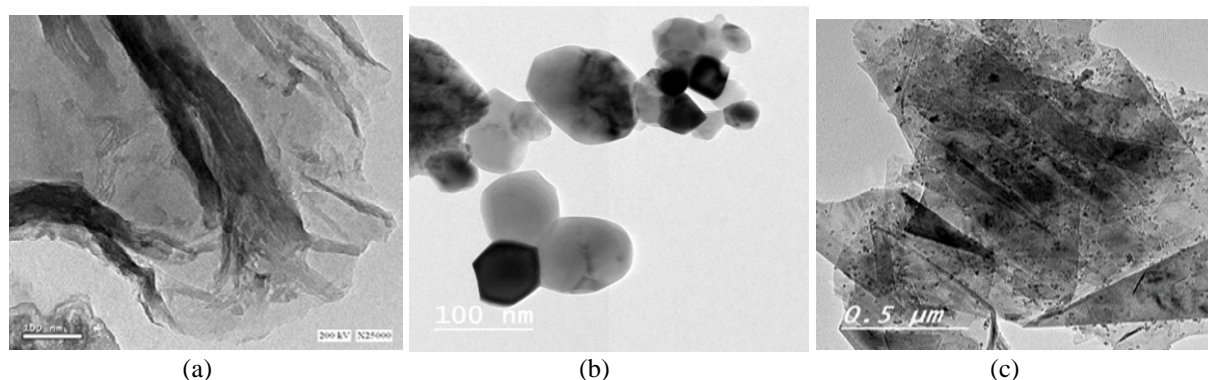
$$E_{ex} = hC/\lambda_{max} \tag{10}$$

(a)   (b)   (c)

Fig. 4. TEM images of (a) reduced grapheme oxide (RGO), (b) pure ZnO, and (c) for the RGO/ZnO nanocomposite.

(a)   (b)

(c)
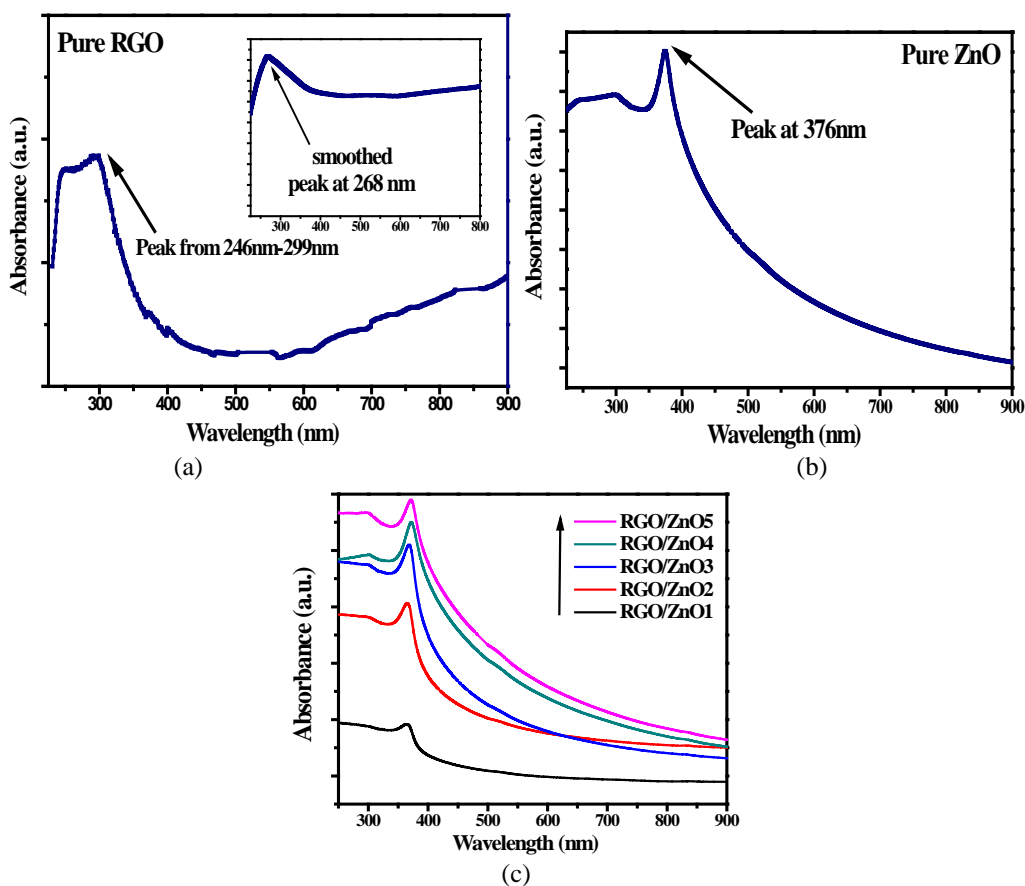
Fig. 5 (a) Absorption versus wavelength spectrum for RGO. The inset shown the smoothed peak at 268 nm, (b) absorption versus wavelength spectrum for pure ZnO, and (c) absorption versus the incident wavelength spectra for RGO/ZnO nanocomposites.

Where h is Planck's constant, C is the velocity of light, and λ_{max} is the exciton peak wavelength. It is shown that increasing ZnO ratio leads to a red shift in both exciton peaks. Usually Tauc's plot is the most verified method for obtaining the optical energy gap.The optical absorption spectra were analyzed according to Tauc`s relation in the form:

$$\alpha h v = B(\alpha h v - E_g)^r \tag{11}$$

Where α is the absorption coefficient, $h v$ is the photon energy, E_g is the optical band gap and B is the steepness or ordering parameter.

The Tauc's relation for direct band gap [24]:

$$(A h v)^2 = B (h v - E_g)^r \tag{12}$$

Where *B* is the edge width parameter, E_g is the optical energy gap of the material, which refer to the direct band gap of optical transitions. Fig. 6 describes the change in Exciton peak with ZnO mass ratio, and obviously show that E_g values are increasing with the increasing ZnO ratio. That can be attributed to the higher E_g value of ZnO when compared with that of RGO as shown in table 3.
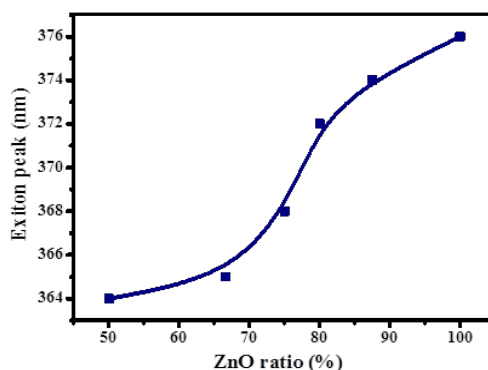
Fig. 6 The dependence of the optical energy gap and the corresponding exciton peak energy on ZnO ratio for RGO/ZnO nanocomposites.

The noticeable increase in E_g and E_{ex} may be described to the increase in the crystallite size due to the improvement in crystallinity by ZnO incorporation in graphene matrix [25]–[28].

The absorption coefficients near the fundamental absorption edge are exponentially dependent on the photon energy, and obey Urbach's empirical relation [29]:

$$\alpha = \alpha_0 exp \left(\frac{h v}{E_e}\right) \tag{13}$$

$$\text{Ln } \alpha = \alpha_o + \left(\frac{h v}{E_e}\right) \tag{14}$$

Where α_0 is a constant and E_e is the Urbach energy which is interpreted as the width of band tail of localized states in the band gap and in general represents the degree of disorder in an amorphous semiconductor. The absorption in this region is due to transitions between extended states in one band and localized states in the exponential tail of the other band.

The photon energy dependence of the absorption coefficient can be described by Urbach's relation given by Eqs. (13, 14). Fig. 7(a) shows a plot of ln(α) versus $h v$ of pure RGO and pure ZnO. Fig. 7(b) shows a plot of ln(α) versus $h v$ of RGO/ZnO nanocomposites. That should give a linear portion with a slope equal to the inverse of E_e and the obtained E_e values are given in Table 3. The E_e values of the RGO/ZnO are increased with increasing ZnO content. One noted that the values of E_e are changed inversely with those of E_g and this may be due to the increase of the disorder of RGO matrix by ZnO doping. This increase leads to distribution of states from band to tail and thus allows for many possible bands to exhibit tail to tail transitions.

Figure 8(a) shows the energy gap determination of pure RGO, Fig. 8(b) shows energy gap determination of pure ZnO and Fig. 8(c) shows the effect of ZnO ratio on energy gap value. Energy gap of ZnO is 3.34 eV and 2.39 eV for reduced graphene oxide, and it's clear that energy gap is gradually increased with the increasing of ZnO content in composites may be energy gap in RGO is lower than the energy gap of ZnO or the increasing in grain size of nanocomposite with increasing in ZnO mass ratio.

The effect of UV irradiation on the absorption spectra and other optical properties was studied by putting diluted solution sample under UV light irradiation and measure the absorbance every half hour as shown in Figs. 9 & 10 for RGO and ZnO, respectively. Increasing UV irradiation dose results in enhancement in the absorption accompanied by a blue shift in E_g values due to induced UV effect.
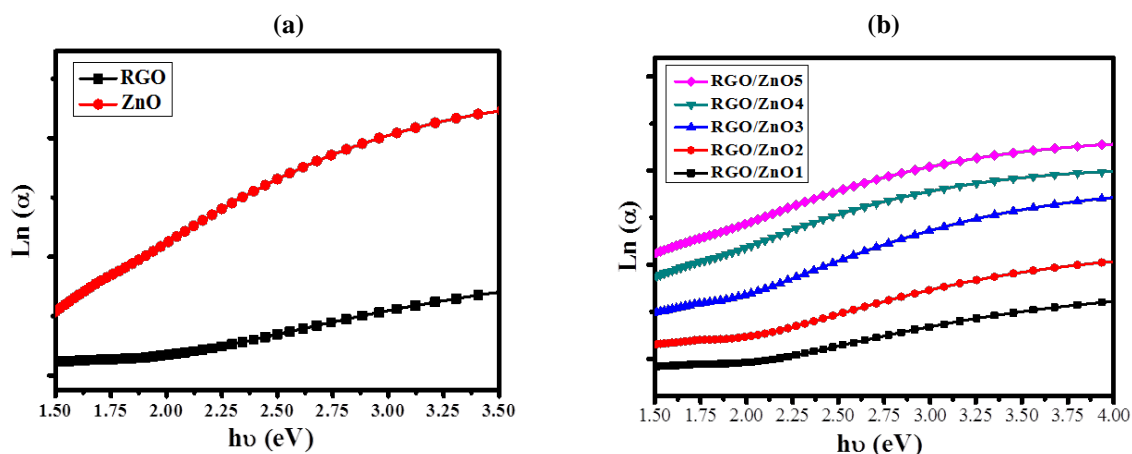
(a)

(b)

Fig. 7 (a) Plot of Ln(α) versus hν of pure RGO and pure ZnO, (b) lnα versus hν for RGO/ZnO nanocomposites.
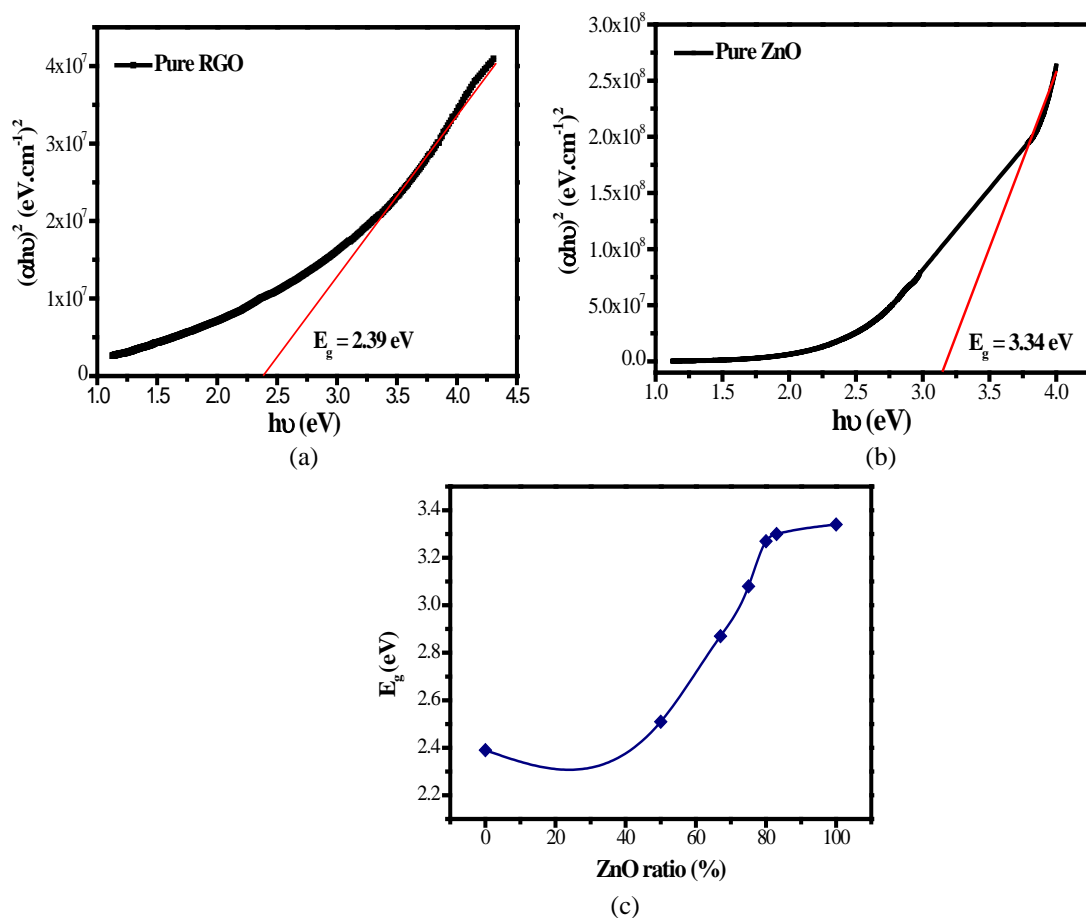

(a)

(b)

(c)

Fig. 8 (a) Energy gap determination of pure RGO, (b) Energy gap determination of pure ZnO, and (c) The dependence of energy gap on ZnO ratio.

Table 3. Exciton peak and energy gap (E_g) for pure ZnO, pure RGO and RGO/ZnO nanocomposites

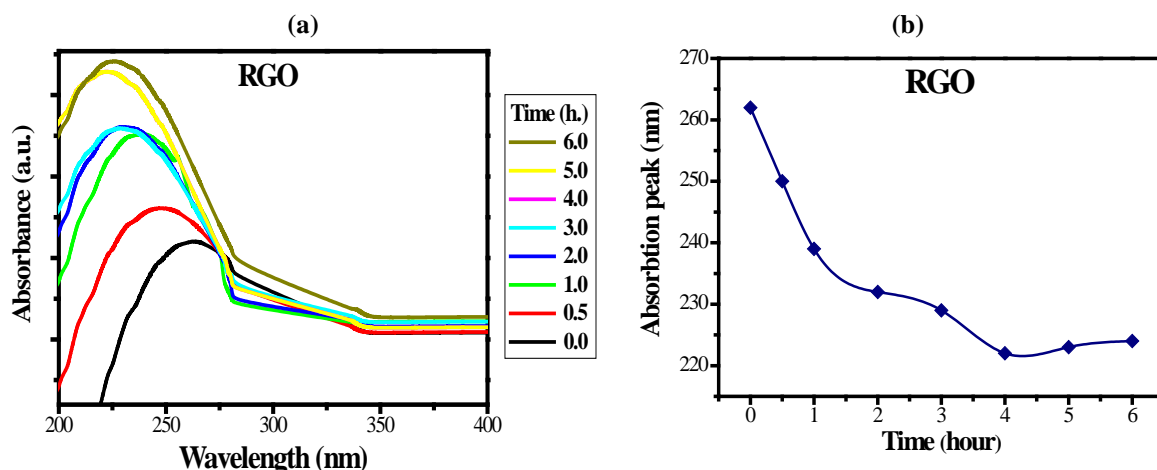| Sample	Exciton peak (nm)	Energy gap (E_g) (eV)
ZnO	376	3.34
RGO	268	2.39
RGO/ZnO1	361	2.51
RGO/ZnO2	365	2.87
RGO/ZnO3	368	3.08
RGO/ZnO4	371	3.27
RGO/ZnO5	372	3.3

(a)   **(b)**

Fig. 9 (a) Effect of UV irradiation dose on the optical absorbance spectra of pure RGO, (b) Effect of UV irradiation dose on the optical absorbance peak of pure RGO.
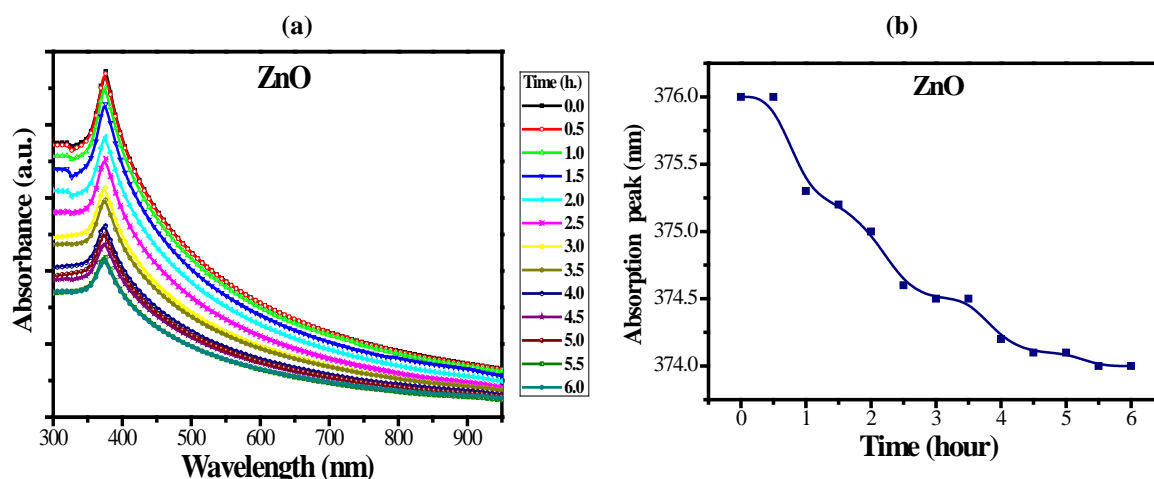
(a)   **(b)**

Fig. 10 (a) Effect of UV irradiation dose on the optical absorbance spectra of pure ZnO, (b) Effect of UV irradiation dose on the optical absorbance peak of pure ZnO.

3.4 FT–IR Spectroscopy

Fourier transforms infrared spectroscopy (FT-IR) is obtained as transmission spectra of KBr sample pellets in order to characterize the bond structure of RGO, ZnO, and RGO/ZnO nanocomposites. Figure 11 shows (FT-IR) of RGO, ZnO, and RGO/ZnO nanocomposites in the range of 4000 to 400 cm^{-1}.

The absorption peak of reduced graphene oxide at the high frequencies centered at 3457 cm^{-1} refers to a large amount of hydroxyl group (O-H) which refer to the moisture in sample this may be from KBr or the sample contain some water remain after drying and also for the peak at 2341 cm^{-1}. A wide spectral peak from 2000 cm^{-1} to 3500 cm^{-1} corresponding to the absorption of water molecules and that indicate the high of moisture of RGO. The transmittance peak at 1122 cm^{-1} represents the (C-O) bonds and (C-OH) on the surface of RGO nanosheets. On the other side, zinc oxide the absorption peak at high frequencies area also refer to the moisture of water molecule such as the peak at 3435 cm^{-1} and the peak at 562 cm^{-1} represent the (Zn-O) bonds as shown in table 4. Figure 11 shows that with increasing in ZnO mass ratio in samples (Zn-O) bond peak is stretched and shifted to left.

4. Conclusions

In summery reduced grapheme oxide (RGO) were synthesized via modified Hummer's method at low temperature process and RGO/ZnO nanocomposites were synthesized via facile low temperature hydrothermal method. It obviously from TEM images that ZnO nanoparticles are homogeneously decorated on the surface of RGO sheets and stack on RGO sheets. The values of the optical energy gap E_g increase with increasing ZnO ratio in RGO/ZnO nanocomposites, while the Urbach tail energy E_e takes the opposite trend. The UV irradiation dose increment introduce an enhancement in the absorption spectral behavior accompanied by a blue shift in the optical energy gap values. FT-IR spectra ensure the formation of nanocomposites. This facile synthesis method can be

easily used to the synthesis of other RGO-based hybrid nanocomposite materials for many purposes such as electrochemical based sensors or photodegradation.
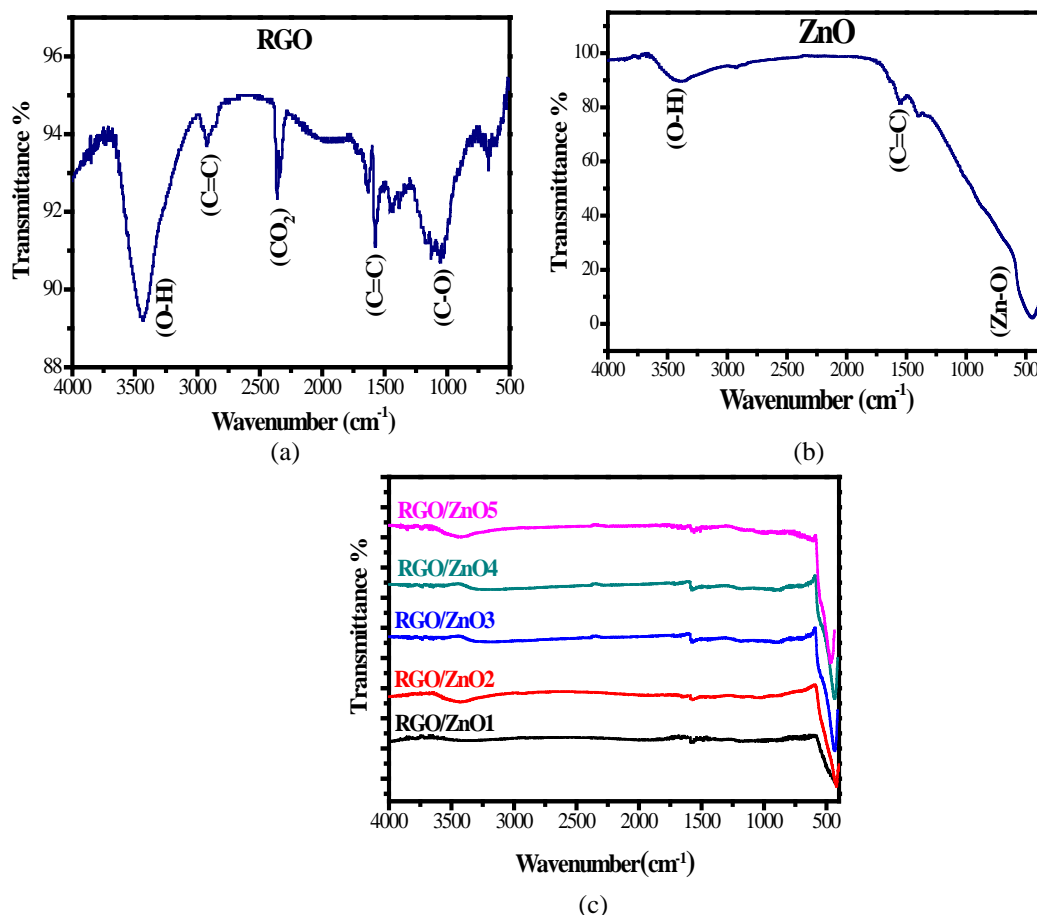

Fig. 11 FT-IR Spectroscopy of (a) pure RGO, (b) Pure ZnO, and (c) RGO/ZnO nanocomposites.

Table 4. FT-IR peaks and their characteristic bonds for ZnO.

FT-IR peak (cm⁻¹)	3435	2993	2861	2359	1635	1401	1122
Bond	O-H	C-H	C-H	CO_2	C=C	C=O	C-O

5. References

[1] Zhang Y, Kang Z, Yan X, Liao Q. ZnO nanostructures in enzyme biosensors. Science China Materials. 2015;58(1):60-76.
[2] Hummers Jr WS, Offeman RE. Preparation of graphitic oxide. Journal of the American Chemical Society. 1958;80(6):1339.
[3] Anand K, Singh O, Singh MP, Kaur J, Singh RC. Hydrogen sensor based on graphene/ZnO nanocomposite. Sensors and Actuators B: Chemical. 2014;195:409-415.
[4] Subramani K, Sathish M. Facile synthesis of ZnO nanoflowers/reduced graphene oxide nanocomposite using zinc hexacyanoferrate for supercapacitor applications. Materials Letters. 2019;236:424-427.
[5] Pumera M. Graphene in biosensing. Materials today. 2011;14(7-8):308-315.
[6] Park JW, Lee C, Jang J. High-performance field-effect transistor-type glucose biosensor based on nanohybrids of carboxylated polypyrrole nanotube wrapped graphene sheet transducer. Sensors and Actuators B: Chemical. 2015;208:532-537.
[7] Xiang Q, Yu J, Jaroniec M. Graphene-based semiconductor photocatalysts. Chemical Society Reviews. 2012;41(2):782-796.
[8] Bolotin KI, Sikes KJ, Jiang Z, Klima M, Fudenberg G, Hone J, Kim P, Stormer HL. Ultrahigh electron mobility in suspended graphene. Solid State Communications. 2008;146(9-10):351-355.
[9] Ning G, Fan Z, Wang G, Gao J, Qian W, Wei F. Gram-scale synthesis of nanomesh graphene with high

surface area and its application in supercapacitor electrodes. Chemical Communications. 2011;47(21):5976-5798.

[10] Stankovich S, Dikin DA, Piner RD, Kohlhaas KA, Kleinhammes A, Jia Y, Wu Y, Nguyen ST, Ruoff RS. Synthesis of graphene-based nanosheets via chemical reduction of exfoliated graphite oxide. Carbon. 2007;45(7):1558-1565.

[11] Lin YM, Avouris P. Strong suppression of electrical noise in bilayer graphene nanodevices. Nano letters. 2008;8(8):2119-2125.

[12] Azarang M, Shuhaimi A, Yousefi R, Golsheikh AM, Sookhakian M. Synthesis and characterization of ZnO NPs/reduced graphene oxide nanocomposite prepared in gelatin medium as highly efficient photo-degradation of MB. Ceramics International. 2014;40(7):10217-10221.

[13] Song SH, Jang MH, Chung J, Jin SH, Kim BH, Hur SH, Yoo S, Cho YH, Jeon S. Highly efficient light‑emitting diode of graphene quantum dots fabricated from graphite intercalation compounds. Advanced Optical Materials. 2014;2(11):1016-1023.

[14] Ezeigwe ER, Tan MT, Khiew PS, Siong CW. One-step green synthesis of graphene/ZnO nanocomposites for electrochemical capacitors. Ceramics International. 2015;41(1):715-724.

[15] Low SS, Tan MT, Loh HS, Khiew PS, Chiu WS. Facile hydrothermal growth graphene/ZnO nanocomposite for development of enhanced biosensor. Analytica Chimica Acta. 2016;903:131-141.

[16] Chia JS, Tan MT, Khiew PS, Chin JK, Lee H, Bien DC, Siong CW. A novel one step synthesis of graphene via sonochemical-assisted solvent exfoliation approach for electrochemical sensing application. Chemical Engineering Journal. 2014;249:270-278.

[17] Li Y, Wang D, Li W, He Y. Photoelectric conversion properties of electrochemically codeposited graphene oxide–ZnO nanocomposite films. Journal of Alloys and Compounds. 2015;648:942-950.

[18] Haghshenas SS, Nemati A, Simchi R, Kim CU. Photocatalytic and photoluminescence properties of ZnO/graphene quasi core-shell nanoparticles. Ceramics International. 2019;45(7):8945-8961.

[19] Ding J, Zhu S, Zhu T, Sun W, Li Q, Wei G, Su Z. Hydrothermal synthesis of zinc oxide-reduced graphene oxide nanocomposites for an electrochemical hydrazine sensor. RSC Advances. 2015;5(29):22935-22942.

[20] Conde MN, Dakhsi K, Zouihri H, Abdelouahdi K, Laanab L, Benaissa M, Jaber B. Preparation of ZnO nanoparticles without any annealing and ripening treatment. Journal of Materials Science and Engineering: A. 2011;1(7A):985.

[21] Scherrer P. Göttinger Nachrichten Math. Phys. 1918;2:98-100.

[22] Williamson GK, Hall WH. X-ray line broadening from filed aluminium and wolfram. Acta Metallurgica. 1953;1(1):22-31.

[23] Kumar S, Sharma P, Sharma V. CdS nanofilms: synthesis and the role of annealing on structural and optical properties. Journal of Applied Physics. 2012;111(4):043519.

[24] Tauc J, Menth A. States in the gap. Journal of Non-Crystalline Solids. 1972;8:569-585.

[25] Kamarulzaman N, Kasim MF, Rusdi R. Band gap narrowing and widening of ZnO nanostructures and doped materials. Nanoscale Research Letters. 2015;10(1):346.

[26] Sarma H, Chakrabortty D, Sarma KC. Structural and optical properties of Zno nano particles. IOSR Journal of Applied Physics. 2014;6(4):08-12.

[27] Joseph SL, John AO, Mugwang'a FK, Katana GG. Tuning the band gap energy of reduced graphene oxide using biopolymer chitosan for high power and frequency device applications. American Journal of Polymer Science & Engineering. 2019;7(1):8-19.

[28] Prabhu S, Pudukudy M, Sohila S, Harish S, Navaneethan M, Navaneethan D, Ramesh R, Hayakawa Y. Synthesis, structural and optical properties of ZnO spindle/reduced graphene oxide composites with enhanced photocatalytic activity under visible light irradiation. Optical Materials. 2018;79:186-195.

[29] Kurik MV. Urbach rule. Physica Status Solidi (A). 1971;8(1):9-45.